IAEA-SM/241-D1

Conf-790507--3

Abstract

The dramatic lowering of fission barriers with increasing angular momentum has provided a firm bridge between the fields of fission and of heavy-ion-induced reactions. The purpose of this review paper is to explore problems of current interest at the intersection of these two fields.

Theoretical considerations of fission of systems with high angular momenta are usually made in the framework of the rotating liquid drop model. The most stringent tests of this theory involve studies of excitation functions for evaporation residue products. At present there is no evidence for the survival of any rotating system which is predicted not to have a fission barrier. The extent to which the vanishing fission barrier imposes a limit on evaporation residue cross sections will be discussed with reference to several cases, ranging from very light systems, such as $^{14}N + ^{12}C$ to medium mass systems, such as $^{86}Kr + ^{65}Cu$.

The prevalence of deeply inelastic processes in heavy ion reactions poses a problem for arriving at an operational definition of heavy-ion-induced fission. This in turn makes it difficult to define fusion of complex nuclei. While some yield at symmetric mass divisions is usually observed and while the products in this region often have fission-like kinetic energies and even angular distributions, indications are that in most cases tails of strongly damped distributions are involved, rather than the fusion-fusion process. This point will be illustrated with reference to the Ne + Ni and Kr + Bi reactions. In some cases, there is strong evidence for the existence of a separate and distinct fission component. Reference will be made to the Ar + Au and Xe + Fe cases.

When excitation functions for both evaporation residue products and for well-characterized fission fragments are available, it is possible to carry out a statistical model analysis and extract values of the fission barrier. Beckerman and Blann have carried out such analyses for systems ranging from $^{35}Cl + ^{62}Ni$ to $^{35}Cl + ^{116}Sn$ and concluded that liquid drop fission barriers must be reduced by $\approx$ 40% to reproduce experimental results. A critical appraisal of this conclusion will be given. New results will be introduced for the compound nucleus $^{153}Tb^*$ obtained from $^{20}Ne + ^{133}Cs$ and $^{12}C + ^{141}Pr$ reactions. These data allow a very stringent test of the theory of angular-momentum dependence of fission barriers.

IAEA-SM/241-D1

Heavy-Ion-Induced Fission Following Fusion*

F. Plasil and R. L. Ferguson
Oak Ridge National Laboratory, Oak Ridge, Tennessee 37830 USA

1. Introduction

The rapid lowering of the fission barrier B_f with increasing angular momentum was first discussed more than 15 years ago [1], and detailed calculations in the framework of the liquid drop model were published in 1974 [2]. It was emphasized [2,3] that the fission barrier is predicted to become zero for all nuclei provided that the angular momentum is sufficiently high; thus, at angular momenta greater than about 100 $\hbar$, no nuclei are expected to have a finite fission barrier. Since angular momenta of 100 $\hbar$ are easily achieved in reactions with heavy ions from present-day facilities, the consequences of the lowering of B_f with increasing angular momentum have aroused considerable interest in recent years. Among the possible consequences, we may consider the following: First, heavy-ion-induced fission may be observable for nuclei in all mass regions; second, cross sections for evaporation residue (ER) products may be limited by the angular-momentum-dependent fission competition; and third, the vanishing fission barriers may imply a limit on the probability of compound nucleus formation and/or on the probability of fusion of the heavy-ion nuclei with those of the target.

In this review paper we shall discuss some of the above effects with reference to experimental results. We shall also discuss quantitative aspects of the angular-momentum dependence of fission barriers, including

---

*Research sponsored by the Division of Physical Research, U. S. Department of Energy, under contract W-7405-eng-26 with Union Carbide Corporation.

the extraction of B_f values from experimental data on heavy-ion-induced fission. In section 2 fission-imposed limits on evaporation residue products will be considered. In section 3 we shall address the question of characterization of heavy-ion-induced fission, and, finally, fission barriers will be discussed in section 4.

2. Cross Section Limits for Evaporation Residue Products

In some sense, comparisons of measured cross sections σ_{ER} for evaporation residue products with theoretical predictions constitute the most stringent tests of the theory of the angular-momentum dependence of fission barriers. This is due to the fact that such tests are essentially independent of the reaction mechanism giving rise to the ER products. Thus if σ_{ER} for any given case were to be found to exceed substantially the predicted $B_f = 0$ limit, nuclei predicted to be unstable against fission would have had to deexcite by particle emission rather than by fission. Such a situation would certainly imply a serious quantitative discrepancy between theory and experiment.

Before reviewing experimental results, we wish to comment on quantitative limitations of the rotating liquid drop theory. As was pointed out in Ref. 2, the liquid drop calculations have been made under the assumption of axial symmetry. This approximation, however, is believed not to lead to serious error, since most of the shapes under consideration are either very elongated or are, in fact, predicted to be axially symmetric (see Ref. 2). A more serious problem can be raised by questioning the validity of the liquid drop model in general. The first point we wish to make in this regard is that the lowering of fission barriers with increasing angular momentum is relatively independent of model assumptions. The basic requirement is that the moment of inertia of the saddle-point shape be significantly

greater than that of the rotating ground state and that this situation persist with increasing angular momentum. Since rotational energy varies inversely with the moment of inertia, the total energy of the saddle-point shape will increase more slowly with increasing angular momentum than the energy of the rotating ground state. Thus the fission barrier, which is the difference between the energies of the two shapes, will decrease. Since the saddle-point shapes are believed to be very elongated in the case of most nuclei and since there is no reason to believe that this situation changes as the angular momentum is increased, the above condition is very probably satisfied.

The second point to be made regarding the validity of the liquid drop model refers to conditions under which single particle effects may dominate. These conditions may apply in the case of systems with relatively few nucleons, where the description of nuclei in liquid drop terms may be inappropriate, as well as in the case of very heavy systems, where shell effects may strongly influence the value of the fission barrier.

In addition to keeping in mind the points mentioned above, it is necessary that we examine only those cases where σ_{ER} is not limited by entrance channel conditions. All these constraints lead us to the region of medium mass nuclei as being the most favorable for comparison between experiment and theory. In Fig. 1 σ_{ER} results are shown for ^{86}Kr bombardments of ^{65}Cu [4]. Theoretical curves were obtained by means of statistical model calculations [5-8] in which angular-momentum dependent fission barriers are included [2]. The experimental points are seen to fall between two extreme assumptions of the approximate statistical model calculation. (In one case evaporated particles are assumed not to change the angular momentum distribution, while in the other case each evaporated neutron decreases the angular momentum by 2 $\hbar$, each proton by 3 $\hbar$, and each ^{4}He by 10 $\hbar$ [8].)

Thus agreement between experiment and theory for this system is good. Similar good agreement is obtained in a number of other cases, including the $^{109}Ag + ^{40}Ar$ reaction of Britt, et al. [9].

If we consider very light systems in spite of the reservations expressed above, we find that σ_{ER} values often approach the liquid drop limit [10-11]. In a recent study, Stokstad, et al. [12-13] investigated the deexcitation of ^{26}Al formed in the reactions $^{10}B + ^{16}O$ and $^{12}C + ^{14}N$. Their results [13] are shown in Fig. 2. While the differences between the two reactions are beyond the scope of this paper, it is interesting to note that both reactions exhibit a remarkable decrease in σ_{ER} as a function of energy at exactly the $B_f = 0$ limit predicted by the rotating liquid drop model [2]. Given the low mass of the ^{26}Al compound nucleus, this striking agreement is perhaps better than one might have expected.

Another interesting case involving the relatively light system $^{16}O + ^{40}Ca$ was investigated recently by Vigdor, et al. [14]. The σ_{ER} values were found to be essentially constant near 1150 mb over an energy range from 40 MeV to 214 MeV. At the highest energy, the ER cross section reached the value calculated to correspond to the $B_f = 0$ limit. Recently, measurements on this system were extended to 316 MeV by Britt, et al. [15], and from preliminary results it appears that the ER cross section is considerably lower than 1150 mb. The decrease is consistent with the predicted $B_f = 0$ limit.

We are not aware of any case in which the measured σ_{ER} values exceed substantially the calculated $B_f = 0$ limit; nevertheless, caution must be used when calculations with liquid drop fission barriers are used to predict evaporation residue cross sections. Such predictions are reasonably reliable only when the non-rotating barrier, B_f^o, is considerably larger than typical particle binding energies. This point is illustrated in

Table I for the reactions $^{65}Cu + {}^{86}Kr$ and $^{109}Ag + {}^{86}Kr$ [4]. The compound nucleus $^{151}Tb^*$ has a calculated value of $B_f^o \approx 33.5$ MeV, while for $^{195}Bi^*$, $B_f^o \approx 11.7$ MeV. It can be seen that in the $^{65}Cu + {}^{86}Kr$ case calculated σ_{ER} values are relatively insensitive to the choice of a_f/a_ν, the ratio of the statistical model level density parameter for fission to that for particle emission. On the other hand, the calculated ER cross sections are very sensitive to the value of the level density parameter ratio in the $^{109}Ag + {}^{86}Kr$ case, and since the a_f/a_ν values in the table all fall within a reasonable range, it is not reliable to use calculated fission barriers and the statistical model to predict σ_{ER} for such a relatively high-Z case.

Thus we may conclude that the liquid drop theory of angular-momentum-dependent fission barriers predicts absolute limits on ER cross sections which are not known to have been exceeded. Furthermore, provided that the non-rotating fission barrier is considerably larger than the particle binding energy, and, provided that entrance channel effects do not limit the fusion cross section, the rotating liquid drop theory gives reasonable predictions for total ER cross sections. Finally, the liquid drop model appears to work even for very light systems such as N + C, at least as far as the limit on σ_{ER} is concerned. In these light cases, σ_{ER} is often observed to be close to that corresponding to the calculated $B_f = 0$ limit.

3. Characterization of Heavy-Ion-Induced Fission

In this section, we will attempt to categorize heavy-ion-induced fission and fission-like phenomena. In early studies of heavy-ion-induced fission, the question of definition of the fission process did not pose a problem. In the systems studied, fission was induced with relatively light heavy ions ranging from C to Ne [15-21], and fission products constituted a well-defined and separated peak in the mass and kinetic energy distributions of reaction

products. The peak in the mass-yield distribution was found to be centered at symmetric mass divisions, and the angular distributions of the fission fragments followed a $1/\sin\theta$ functional form. The kinetic energies were understood in terms of Coulomb repulsion between the elongated nascent fragments at the time of scission, and it was concluded from all indications that fission followed compound nucleus formation. Empirically, the four observable conditions characterizing fission are: (i) a distinct peak in the mass (or charge) yield distribution of products that is centered at symmetric mass divisions; (ii) a $1/\sin\theta$ angular distribution; (iii) a predictable fragment kinetic energy distribution [22]; and (iv) full momentum transfer from the projectile to the fissioning system (as determined by angular correlation measurements [16,20,23]).

Conceptually, fission following compound nucleus formation is certainly a well-defined process. Target and projectile nuclei fuse with each other, the system equilibrates in all degrees of freedom while undergoing several rotations, and fission finally takes place during the deexcitation process if it has successfully competed with particle emission. In practice, compound nucleus formation may be difficult to achieve in systems with very high excitation energies and angular momenta, since the composite system of target and projectile is likely to have a short lifetime and may begin to deexcite by particle emission even before equilibrium in all degrees of freedom has been achieved. We shall refer to the fission of a fused composite system as fusion-fission (FF). Thus compound nucleus fission, CNF, is a special case of FF; namely, one in which equilibrium in all degrees of freedom has taken place prior to fission. While FF in general may satisfy all of the fission conditions listed above, a statistical model treatment is applicable only to CNF.

Before giving examples of experimental results, we would like to describe one more reaction category which may give rise to fission-like products, namely, deeply inelastic collisions, DIC. These have been very successfully described in terms of diffusion models. In many cases, when the collision time is sufficiently long, diffusion processes may involve sufficient mass and charge transfer so that DIC products can be observed in the same mass region as FF products. Since the time associated with the tail of the DIC distribution may be similar to the time relevant to FF, the distinction between FF and the DIC tail may be only academic. It is unlikely, however, that DIC will result in a peak in the mass distribution centered at symmetric mass divisions (except, of course, in those cases when the target and projectile have nearly equal masses), and thus distributions of products resulting from DIC will in general not satisfy fission condition (i) listed above.

By way of illustrating the above discussion, we shall first consider fission events resulting from reactions with relatively light heavy ions such as Ne. An example of raw data in which the fission products stand out clearly is shown in Fig. 3 for the case of $^{20}Ne + ^{150}Nd$ [24]. The fission events form a separate peak at relatively high values of ΔE and medium values of E. From the kinetic energy measurement and from studies of similar systems, it can be concluded that the fission peak shown in Fig. 3 is definitely a result of FF and is very probably due to CNF.

A quite different picture emerges for the case of $^{20}Ne + Ni$ [25]. In Fig. 4 the overall charge distribution of the lighter reaction products is shown. Since the composite system has Z = 38, symmetric charge divisions correspond to Z = 19, or about 2 units of charge less (Z = 17) if evaporation from the composite system and/or from the products is taken into account. It is clear that there is no hint of a peak at symmetric

charge divisions. On the other hand, other conditions characterizing fission are satisfied. For example, the angular distributions shown in Fig. 5 are given in terms of $d\sigma/d\theta_{cm}$, and thus a constant distribution implies a $1/\sin\theta$ functional form. It can be seen that for products with $Z \gtrsim 15$ this condition is satisfied. In Fig. 6, the kinetic energy of the observed reaction products is plotted as a function of Z. Theoretical predictions for kinetic energies of fission fragments, derived from the work of Davies, et al. [22], are indicated by the curve. When the theoretical calculations are corrected for particle emission from the excited fragments, the open circles are obtained. For $Z \gtrsim 15$, the calculated fission fragment energies are in excellent agreement with measured values. Thus the case of ^{20}Ne + Ni constitutes a typical example of a system in which the tail of the deeply inelastic products extends to the region of symmetric charge divisions, and in which the characteristic properties of the near-symmetric products, such as angular distributions and kinetic energies, are identical to those expected for FF. As was discussed above, whether or not these events are due to DIC or FF is perhaps a matter of personal preference, since on the one hand the near-symmetric events display fission characteristics, while on the other hand, these characteristics evolve smoothly from the deeply inelastic properties. It is unlikely, however, that compound nucleus formation was involved in this case, and thus the events observed are very probably not due to CNF.

An intermediate case between the CNF of Ne + Nd and the DIC of Ne + Ni is the case of Ne + Ag [26]. The charge distributions at several angles and at two bombarding energies are shown in Fig. 7. At the lower bombarding energy there appears a peak at near-symmetric charge splits, but it is not well separated from the deeply inelastic events. At the higher energy, the peak is even less distinct. Babinet, et al. [26] have interpreted the data of Fig. 7, in terms of the diffusion model, but in view of the fact that at

near-symmetric charge divisions the kinetic energies and angular distributions of the products satisfy the FF criteria, and since a distinct peak in the charge yield curve does exist, it is possible that products with $Z \gtrsim 16$ consist of a mixture of DIC and CNF events. The washing out of the peak in the charge distribution with increasing bombarding energy is consistent with this point of view.

Turning to reactions with heavier ions, it is possible, once again, to find examples in which a distinct fission component appears, as well as examples where yield at symmetric mass or charge splits may be associated with tails of distributions of DIC products. In Fig. 8, a mass-energy distribution is shown for the reaction 201-MeV ^{40}Ar + ^{197}Au [27]. The various types of reaction products are identified in the figure, and it can be seen that fission events form a well-defined peak, separated from other events. This case may be contrasted with ^{84}Kr + ^{209}Bi data shown in Fig. 9 [28]. Mass distributions derived from coincidence measurements are shown at 34° and 59°. Once again, there is no peak at near-symmetric mass divisions, and the yield in that mass region appears to be due to a tail of the DIC events. The reason that the yield at symmetric mass division appears only at 59° and not at 34° is probably due to the fact that events appearing at 59° involve longer reaction times than those appearing at 34° and allow more mass transfer. This view is supported by the somewhat lower total kinetic energy associated with the 59° data (275 MeV, compared to 290 MeV at 34°), which implies a greater degree of energy damping.

The final point we wish to make in this section concerns very fissile systems, in which the total fission cross section exceeds the $B_f = 0$ limit. Two such examples are the ^{20}Ne + ^{235}U system studied by Viola, et al. [23] using the angular correlation technique and the ^{132}Xe + ^{56}Fe system of Heusch, et al. [29]. In both of these cases the fission events satisfy

all criteria for FF listed earlier in this section, and in both cases the FF cross section exceeds substantially the $B_f = 0$ limit discussed in section 2. The three possible conclusions that can be drawn from these results are: (i) while all of the fragments observed result from FF, only some are the products of CNF; (ii) compound nuclei with $B_f = 0$ are able to exist; and (iii) the calculated $B_f = 0$ limit is inaccurate, and the true $B_f = 0$ limit corresponds to a higher fission cross section. Of the three alternatives given above, (iii) seems unlikely to be correct in view of the considerations given in section 2. On the other hand, alternative (i), namely, that not all observed fission fragments result from CNF, is very likely to be true, and thus the description of a "new type of strongly damped collision" evolved in Ref. 29 to explain the Xe + Fe data may not be necessary.

We conclude this section by pointing out that if we wish to restrict our attention to compound nucleus fission we should consider only fissioning systems with $130 \lesssim A \lesssim 210$, and only those cases in which fission was induced by ions with $A \lesssim 40$.

4. Fission Barriers from Heavy Ion Reactions

In this section we examine problems associated with the extraction of fission barriers from excitation functions for heavy-ion-induced reactions. In view of the discussion of the previous section as to which cases constitute CNF, it is clear that considerable care must be exercised in choosing appropriate fissioning systems. First, systems to be used for the determination of fission barriers must not be dominated by DIC products. This excludes such light systems as the Ne + Ni case discussed in section 3, as well as the ^{35}Cl + Ni case considered by Beckerman and Blann [30]. Systems in which target and projectile masses are similar are also unsuitable,

since it is not possible in these cases to separate CNF from DIC products. An example of such a case is the $^{65}Cu + ^{86}Kr$ data of Ref. 9. This same difficulty applies to cases in which fission-like events consist of a mixture of DIC and CNF products and in which the separation into two distinct components is ambiguous. Examples of such cases are the Ag + Ne data discussed in the previous section, as well as the $^{40}Ar + ^{109}Ag$ data of Britt, et al. [9], which were used by Beckerman and Blann [30] to determine the fission barrier of the compound nucleus ^{149}Tb. Finally, very fissile systems such as the $^{20}Ne + ^{235}U$ of Viola, et al.[23] are also not appropriate. While they almost certainly involve FF, it is probable that not all of the events result from CNF, and thus they do not lend themselves to a statistical model analysis. With all of the above constraints, we are restricted to cases in which fission is induced by relatively light heavy ions such as C and Ne and to systems in the mass range $130 \lesssim A \lesssim 210$.

The most important region of the fission excitation function for the purpose of extracting fission barriers is, not surprisingly, the steep part of the excitation function in the threshold region. This point is discussed and illustrated in Ref. 31 and has been confirmed from an examination of a large number of systems for which data are available. It was found that the value of B_f is determined primarily by the slope of the σ_f function and that poor fits at higher excitation energies did not affect extracted B_f values. It was also found by Moretto, et al. [32] that for ^4He- and proton-induced-fission, fits to entire excitation functions can be obtained over a wide energy range, provided that level densities are based on realistic single particle schemes and that energy-dependent pairing effects are included. Fission barriers extracted by Moretto, et al.[32], however, do not differ substantially from those extracted by Khodai-Joopari [33] on the basis of a statistical model using Fermi gas level densities.

In this work, we have used Fermi gas level densities, and the angular momentum variation of the fission barriers (but not their absolute values) was assumed to be that given by the rotating liquid drop model [2]. The procedure of obtaining statistical model fits to heavy-ion-induced fission excitation functions allowing B_f^o and a_f/a_ν to be free parameters has been described earlier [3,30]. In Refs. 3 and 30 the computer code ALICE [34] was used in this type of analysis. Here, we shall use a recently updated version of the code, ORNL ALICE [7]. Since ALICE-type calculations essentially divide the compound nucleus σ_{CN} cross section into its evaporation residue, σ_{ER}, and fission, σ_f, components, measured values of σ_{ER} are needed along with σ_f values. By assuming that $\sigma_{CN} = \sigma_{ER} + \sigma_f$, it is then possible to apply the statistical model treatment.

Finally, in order to isolate angular momentum effects and in order to provide a stringent consistency check, it is desirable to obtain excitation functions for two systems leading to the same compound nucleus. This motivated us to study the systems $^{12}C + ^{14}Pr$ and $^{20}Ne + ^{133}Cs$, both leading to the compound nucleus ^{153}Tb [35]. The fission data for these systems were dicussed earlier [3], but it is only recently that we have succeeded in measuring the σ_{ER} values needed for an unambiguous statistical model analysis. The σ_{ER} measurements indicate that for Ne + Cs σ_{CN} is approximately equal to the geometric cross section, while for C + Pr σ_{CN} is equal to about 63% of the geometric cross sections.

The fission excitation functions for the two systems are shown in Fig. 10. The effect of the increased angular momentum in the Ne + Cs case is clearly reflected in its enhanced fissility. As was stated above, the fission barrier for the non-rotating system, B_f^o, is determined from the slope of the σ_f function. This is shown in Fig. 11. A number of different fits has been made to the data point at the lowest energy, with B_f^o values

ranging from the liquid drop value $B_{f,LD}^{o}$ to 0.7 $B_{f,LD}^{o}$. The corresponding a_f/a_ν values needed to obtain the fits ranged from 0.985 for 0.7 $B_{f,LD}^{o}$ to 1.245 for $B_{f,LD}^{o}$. It is clear that a fission barrier of 80% of the liquid drop value best fits the observed results. For 0.8 $B_{f,LD}^{o}$, a_f/a_ν was found to be 1.06. In Fig. 12 a fit with 0.8 $B_{f,LD}^{o}$ and a_f/a_ν = 1.0 is shown for the ^{20}Ne + ^{133}Cs case. It can be seen that the fit is excellent, and, as in the case of ^{12}C + ^{141}Pr, it was also found to be unique. Thus it seems reasonable to conclude that the fission barrier of the ^{153}Tb compound nucleus is 80% of the liquid drop value. This conclusion is consistent with the calculations of Krappe and Nix [36].

One troublesome feature of the above fits is that the value of a_f/a_ν is not the same in the two cases; whereas it might have been expected to be identical. The reason for this may be due to errors arising from the σ_{CN} values used in the calculations. In our recent work, it was found that the ratio $\sigma_{ER}/\sigma_{geometric}$ for Ne + Cs is approximately equal to 1.0, while for C + Pr it is equal to 0.63. The corresponding ratio of a_f/a_ν for C + Pr to that for Ne + Cs is 1.06. In Ref. 3, in which $\sigma_{ER}/\sigma_{geometric}$ was assumed to be 1.0 for both systems, the ratio of a_f/a_ν for C + Pr to that for Ne + Cs was found to be 0.97. Thus neither here nor in Ref. 3 was a_f/a_ν found to be the same for the two systems studied, but while it was calculated to be smaller for C + Pr than for Ne + Cs in Ref. 3, the reverse appears to be true in the more recent work. In any case, it is gratifying that the same conclusion was obtained in Ref. 3 as was obtained here: the fission barrier of ^{153}Tb is 80% of the liquid drop value. The fits obtained in Ref. 3 are shown in Fig. 13.

The kinds of problems that may emerge when we attempt to fit data that consist of a mixture of CNF and DIC products are illustrated in Fig. 14 for the case of Ne + Ag [3,37]. Attempted fits to the lowest energy data point

are shown with B_f^o values as low as 60% of $B_{f,LD}^o$. It is clear that it is not possible to obtain a fit to the data over a reasonable range (about 25 MeV) of excitation energy. (An earlier fit reported by Beckerman and Blann [30] to the Ne + Ag data made use of reported [3] σ_{ER} values that were recently found to be in gross error [38].) The reason for this failure is almost certainly that the DIC component, which has been shown to be present, does not vary with excitation energy at the same rate as CNF, and thus the data are not suitable for B_f^o extraction.

In Ref. 30, Beckerman and Blann have concluded that, based on an analysis of five different systems, fission barriers appear to be 50-70% of the liquid drop values. This discrepancy seems surprisingly large, and it is necessary to examine each system involved individually to determine its validity. We have already pointed out that in the case of three of the five systems, namely, Cl + Ni, Ne + Ag and Ar + Ag, there is a strong DIC component present that makes the analysis ambiguous at best.

We have examined in some detail the case of $^{35}Cl + ^{116}Sn$, one of the two remaining systems of Ref. 30. The data are shown in Fig. 15 together with the MB-II fit of Ref. 30, in which final angular momentum states were treated explicitly (solid curve). While in ALICE calculations angular momentum is treated only approximately, it can be concluded from Ref. 30 that adequate fits can nevertheless be obtained with ALICE. This is also shown in Fig. 15 (dashed curve), and we shall thus continue to use ALICE to illustrate the following point. In Ref. 3 it was pointed out that a possible severe source of error in the case of relatively light systems may be the sharp cutoff approximation. In Fig. 15 we show the results for a diffuse cutoff in the angular momentum distribution of the deexciting compound nuclei (dash-dot curve). It can be seen that this calculated fission excitation function lies above the sharp cutoff ALICE result, but that the slope

is changed only slightly. This implies that a diffuse cutoff does not lead to significantly different values of B_f^o. This same conclusion was reached by Blann [39] and co-workers.

Also shown in Fig. 15 is the result using a Monte Carlo-type program PACE, which does take final angular momentum states specifically into account [40] (dotted curve). Since all of the calculations of Fig. 15 involve the same parameters, the relatively large difference between our Monte Carlo-type calculation and that of Ref. 30 is not understood. Since the slope of our calculation is less steep than that of the fit of Ref. 30, it is possible that, if our results are correct, the B_f^o is not as low as the MB-II calculation would imply. The final point to be made is that the Cl data considered by Beckerman and Blann span a rather narrow range of excitation energy (about 12 MeV), compared to an excitation energy range about twice as large for our ^{153}Tb system.

In concluding this section, we wish to observe that, based on the study of the ^{153}Tb system formed in two different ways and over a fairly large range of excitation energies, the fission barriers in this mass region are probably lower than those calculated from the liquid drop model, but only by about 20%, and not the 30-50% deduced earlier.

5. Concluding Remarks

We have shown that the rapid decrease of fission barriers with increasing angular momentum has important implications for heavy-ion-induced fission. Currently, there appear to be no cases in which measured evaporation residue cross sections appreciably exceed the $B_f = 0$ limit. This gives us considerable confidence in the quantiative aspects of current fission theory. The characterization of fission is complicated by the fact that experimentally it is impossible to distinguish between fission following fusion in general, and

the fission of compound nuclei specifically. Furthermore, tails of deeply inelastic reactions may extend into the fission region, and these two types of products may also be indistinguishable from one another. Thus caution must be used when fission barriers are extracted from heavy-ion-induced fission data. However, we have concluded that, in the region of $A \tilde{\sim} 150$, fission barriers have values of about 80% of the liquid drop values and not the 50-70% indicated earlier.

6. Acknowledgements

We are grateful to our colleagues, R. L. Hahn, F. E. Obenshain, F. Pleasonton, A. H. Snell, and G. R. Young for permission to use unpublished experimental data. We wish to thank A. Gavron for modifying the program JULIAN to run in our computer environment and for helpful guidance in using it. Fruitful discussions with M. Blann and M. Beckerman are gratefully acknowledged.

Much of our own experimental work discussed in this paper was done when production of Ne beams at the Oak Ridge Isochronous Cyclotron was far from routine. The skill and dedication of Gene A. Palmer in operating the Cyclotron was especially appreciated, and his untimely death has saddened all of those who knew him.

REFERENCES

[1] COHEN, S., PLASIL, F., SWIATECKI, W. J., Proceedings Third Conference on Reactions Between Complex Nuclei (GHIORSO, A., DIAMOND, R. M., CONZETT, H. E., Eds.), University of California Press, Berkeley (1963) 325; University of California Radiation Laboratory preprint UCRL-10775 (1963).

[2] COHEN, S., PLASIL, F. SWIATECKI, W. J., Ann. Phys. 82 (1974) 557.

[3] PLASIL, F., Proceedings of the International Conference on Reactions Between Complex Nuclei (ROBINSON, R. L., McGOWAN, F. K., BALL, J. B., HAMILTON, J. H., Eds.), North-Holland Publishing Co., Amsterdam (1974) 107.

[4] PLASIL, F., FERGUSON, R. L., BRITT, H. C., ERKKILA, B. H., GOLDSTONE, P. D., STOKES, R. H., GUTBROD, H. H., Phys. Rev. C 18 (1973) 2603.

[5] BLANN, M., PLASIL, F., Phys. Rev. Lett. 29 (1972) 303.

[6] PLASIL, F., BLANN, M., Phys. Rev. C 11 (1975) 508.

[7] PLASIL, F., ORNL ALICE A Statistical Model Computer Code Including Fission Competition, Oak Ridge National Laboratory Report ORNL/TM-6054 (1977).

[8] PLASIL, F., Phys. Rev. C 17 (1978) 832.

[9] BRITT, H. C., ERKKILA, B. H., STOKES, R. H., GUTBROD, H. H., PLASIL, F., FERGUSON, R. L., BLANN, M., Phys. Rev. C 13 (1976) 1483.

[10] NATOWITZ, J. B., CHULICK, E. T., NAMBOODIRI, M. N., Phys. Rev. Lett. 31, (1973) 643.

[11] NAMBOODIRI, M. N., CHULICK, E. T., NATOWITZ, J. B., KENEFICK, R. A., Phys. Rev. C 11 (1975) 401.

[12] STOKSTAD, R. G., DAYRAS, R. A., GOMEZ DEL CAMPO, J., STELSON, P. H., OLMER, C., ZISMAN, M. S., Phys. Lett. 70B (1977) 289.

[12] GOMEZ DEL CAMPO, J., DAYRAS, R. A., BIGGERSTAFF, J. A., SHAPIRA, D., SNELL, A. H., STELSON, P. H., STOKSTAD, R. G., Formation of ^{26}Al by the Reactions ^{10}B + ^{16}O and ^{12}C + ^{14}N, preprint (1979).

[14] VIGDOR, S. E., KOVAR, D. G., SPERR, P., MAHONEY, J., MENCHACA-ROCHA, A., OLMER, C., ZISMAN, M. S., Bull. Am. Phys. Soc. 23 (1978) 615, and preprint (1978).

[15] GORDON, G. E., LARSH, A. E., SIKKELAND, T., SEABORG, G. T., Phys. Rev. 120 (1960) 1341.

[16] SIKKELAND, T., HAINES, E. L., VIOLA, V. E., JR., Phys. Rev. 125 (1962) 1350.

[17] VIOLA, V. E., JR., SIKKELAND, T., Phys. Rev. 128, (1962) 767.

[18] VIOLA, V. E., JR., SIKKELAND, T., Phys. Rev. 130 (1963) 2044, and SIKKELAND, T., Phys. Lett. 31B (1970) 451.

[19] SIKKELAND, T., Phys. Rev. 135 (1964) B669.

[20] SIKKELAND, T., Phys. Lett. 27B (1963) 277.

[21] SIKKELAND, T., CLARKSON, J. E., STEIGER-SHAFRIR, N. H., VIOLA, V. E., JR., Phys. Rev. C 3 (1971) 329.

[22] DAVIES, K. T. R., SIERK, A. J., NIX, J. R., Phys. Rev. C 13 (1976) 2385.

[23] VIOLA, V. E., JR., CLARK, R. G., MEYER, W. G., ZEBELMAN, A. M., SEXTRO, R. G., Nucl. Phys. A261 (1976) 174.

[24] HALBERT, M. L., DAYRAS, R.A., FERGUSON, R. L., PLASIL, F., SARANTITES, D. G., Phys. Rev. C 17 (1978) 155.

[25] OBENSHAIN, F. E., FERGUSON, R. L., HALBERT, M. L., HENSLEY, D. C., NAKAHARA, H., PLASIL, F., PLEASONTON, F., SNELL, A. H., STOKSTAD, R. G., Phys. Rev. C 18 (1978) 764.

[26] BABINET, R., MORETTO, L. G., GALIN, J., JARED, R., MOULTON, J., THOMPSON, S. G., Nucl. Phys. A258 (1976) 172.

[27] NGÔ, C., PÉTER, J., TAMAIN, B., BERLANGER, M., HANAPPE, F., Z. Phys. A 283 (1977) 161.

[28] WOLF, K. L., UNIK, J. P., HUIZENGA, J. R., BIRKELUND, J., FREIESLEBEN, H., VIOLA, V. E., JR., Phys. Rev. Lett. 33 (1974) 1105.

[29] HEUSCH, B., VOLANT, C., FREIESLEBEN, H., CHESTNUT, R. P., HILDENBRAND, K. D., PÜHLHOFER, F., SCHNEIDER, W. F. W., KOHLMEYER, B., PFEFFER, W., Z. Phys. A 288 (1978) 391.

[30] BECKERMAN, M., BLANN, M., Phys. Lett. 68B (1977) 31.

[31] BURNETT, D. S., GATTI, R. C., PLASIL, F., PRICE, P. B., SWIATECKI, W. J., THOMPSON, S. G., Phys. Rev. 134 (1964) B956.

[32] MORETTO, L. G., THOMPSON, S. G., ROUTTI, J., GATTI, R. C., Phys. Lett. 38B (1972) 471.

[33] KHODAI-JOOPARI, Ph. D. Thesis, University of California, Lawrence Radiation Laboratory Report UCRL-16489 (1966).

[34] BLANN, M., PLASIL, F., ALICE: A Nuclear Evaporation Code, U.S.A.E.C. Report COO-3494-10 (1973).

[35] PLASIL, F., FERGUSON, R. L., HAHN, R. L., OBENSHAIN, F. E., PLEASONTON, F., SNELL, A. H., YOUNG, G. R., to be published.

[36] KRAPPE, H. J., NIX, J. R., Proceedings of the Third Symposium on the Physics and Chemistry of Fission 1, International Atomic Energy Agency, Vienna (1974) 159.

[37] PLASIL, F., FERGUSON, R. L., PLEASONTON, F., Proceedings of the Third Symposium on the Physics and Chemistry of Fission 2, International Atomic Energy Agency, Vienna (1974) 319.

[38] PLASIL, F., FERGUSON, R. L., OBENSHAIN, F. E., SNELL, A. H., YOUNG, G. R., to be published.

[39] BLANN, M., private communication (1979).

[40] GAVRON, A., PACE, a Modification of: HILLMAN, M., EYAL, Y., "JULIAN: A Monte-Carlo Hauser-Feshbach Program for Evaporation from Compound Nuclei," Symposium on Neutron Cross Sections from 10 to 40 MeV (BHAT, M. R., PEARLSTEIN, S., Eds.), Brookhaven National Laboratory Report BNL-NCS-50681 (1977) 539; private communication, 1978.

Table I. Effects of Level Density Parameter Variation of Calculated Evaporation Residue Cross Sections.

a_f/a_ν	$^{65}Cu + ^{86}Kr$ (mb)	$^{109}Ag + ^{86}Kr$ (mb)
1.0	245	76.1
1.01	243	59.1
1.05	216	8.70
1.10	173	0.0024

Figure Captions

Fig. 1. Experimental and theoretical excitation functions for evaporation residue products from the system $^{65}Cu + ^{86}Kr$. The difference between the two theoretical curves is discussed in the text. An estimate of the total reaction cross section σ_R is also shown. From Ref. [4].

Fig. 2. Fusion cross sections vs. $1/E_{cm}$ for the systems $^{16}O + ^{10}B$ and $^{14}N + ^{12}C$. The steeply sloping solid line appearing at $1/E_{cm}$ values of $\lesssim 0.02$ MeV^{-1} corresponds to the predicted liquid drop limit for $B_f = 0$. From Ref. [13].

Fig. 3. ΔE vs. E map for the system ^{150}Nd + 175-MeV ^{20}Ne. The principal reaction-product groupings are labeled. From Ref. [24].

Fig. 4. Production cross section vs. Z for the system Ni + 164-MeV ^{20}Ne. From Ref. [25].

Fig. 5. Production cross sections vs. θ_{cm} for various elements from the system Ni + 164-MeV ^{20}Ne. Flat distributions for $Z \gtrsim 15$ in this plot indicate an angle-equilibrated $1/\sin\theta$ functional form. From Ref. [25].

Fig. 6. Experimental and theoretical kinetic energies for products from the reaction Ni + 164-MeV ^{20}Ne. The filled points are the experimental single-fragment kinetic energies in the center-of-mass system; the theoretical curve is derived from Ref. [22]; the open points are the theoretical results corrected for evaporation. From Ref. [25].

Fig. 7. Production cross sections vs. Z at various laboratory angles for the system Ag + ^{20}Ne. From Ref. [26].

Fig. 8. Kinetic energy vs. mass contour diagram of products from the system ^{197}Au + 201-MeV ^{40}Ar. Principal reaction-product groupings are labeled. From Ref. [27].

Fig. 9. Relative mass yields for DIC products from the system ^{209}Bi + 600-MeV ^{84}Kr at two laboratory angles. Average kinetic energies of products detected at 34° and 59° are 290 MeV and 275 MeV, respectively. From Ref. [28].

Fig. 10. Fission excitation functions for fission of the ^{153}Tb compound nucleus produced in two different reactions.

Fig. 11. Experimental and theoretical fission excitation functions for the system $^{141}Pr + ^{12}C$. The curves, which are fit to the lowest energy point, are labeled with the fraction of the liquid-drop fission barrier used in the fit (see text). The best fit was obtained with 0.8 $B^{o}_{f,LD}$ and $a_f/a_\nu = 1.06$.

Fig. 12. Experimental and theoretical fission excitation functions for the system $^{133}Cs + ^{20}Ne$. The theoretical curve is fit to the lowest energy point using 0.8 $B^{o}_{f,LD}$ and $a_f/a_\nu = 1.0$.

Fig. 13. Experimental and theoretical fission excitation functions for fission of the ^{153}Tb compound nucleus produced in two different reactions. The fits are those from Ref. [3] with the assumption that $\sigma_{ER}/\sigma_{geometric} = 1.0$ for both systems (see text).

Fig. 14. Experimental and theoretical fission excitation functions for the system $^{107}Ag + ^{20}Ne$. Theoretical curves, fit to the lowest energy data point, are labeled with the fraction of the liquid-drop fission barrier used in the fit (see text). Experimental data are from Refs. [3,37].

Fig. 15. Experimental and theoretical fission excitation functions for the system $^{116}Sn + ^{35}Cl$. The data and the solid curve (a fit using the program MD-II) are from Ref. 30. The dashed curve is a fit using the program ALICE, and the dash-dot curve shows the result of using a diffuse cutoff in the angular momentum distribution. The dotted curve represents a calculation using the program PACE of Ref. 40.

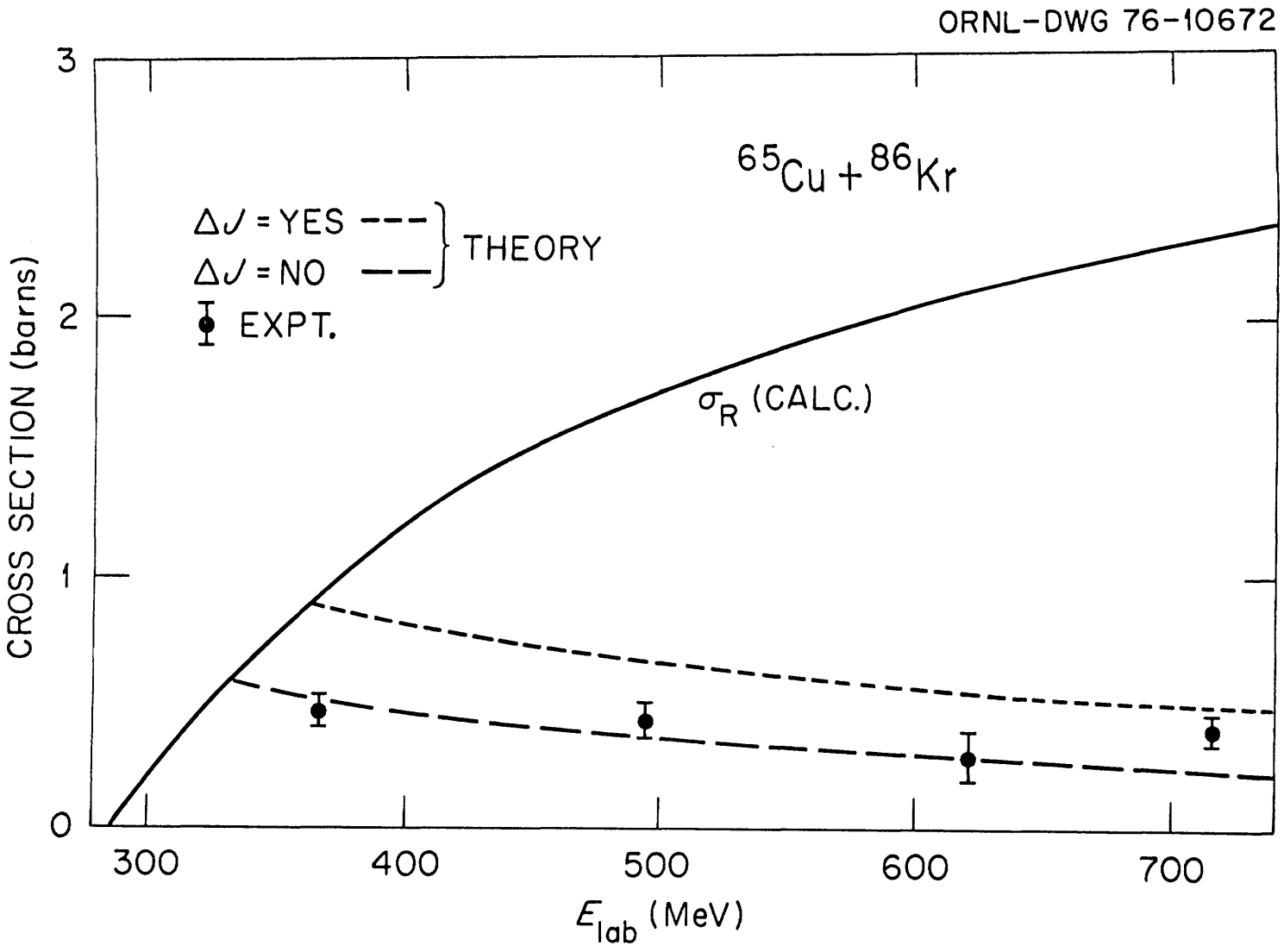
ORNL-DWG 76-10672
$^{65}Cu + ^{86}Kr$
ΔJ = YES
ΔJ = NO
THEORY
EXPT.
σ_R (CALC.)
CROSS SECTION (barns)
E_{lab} (MeV)
0
1
2
3
300
400
500
600
700

Fig. 1

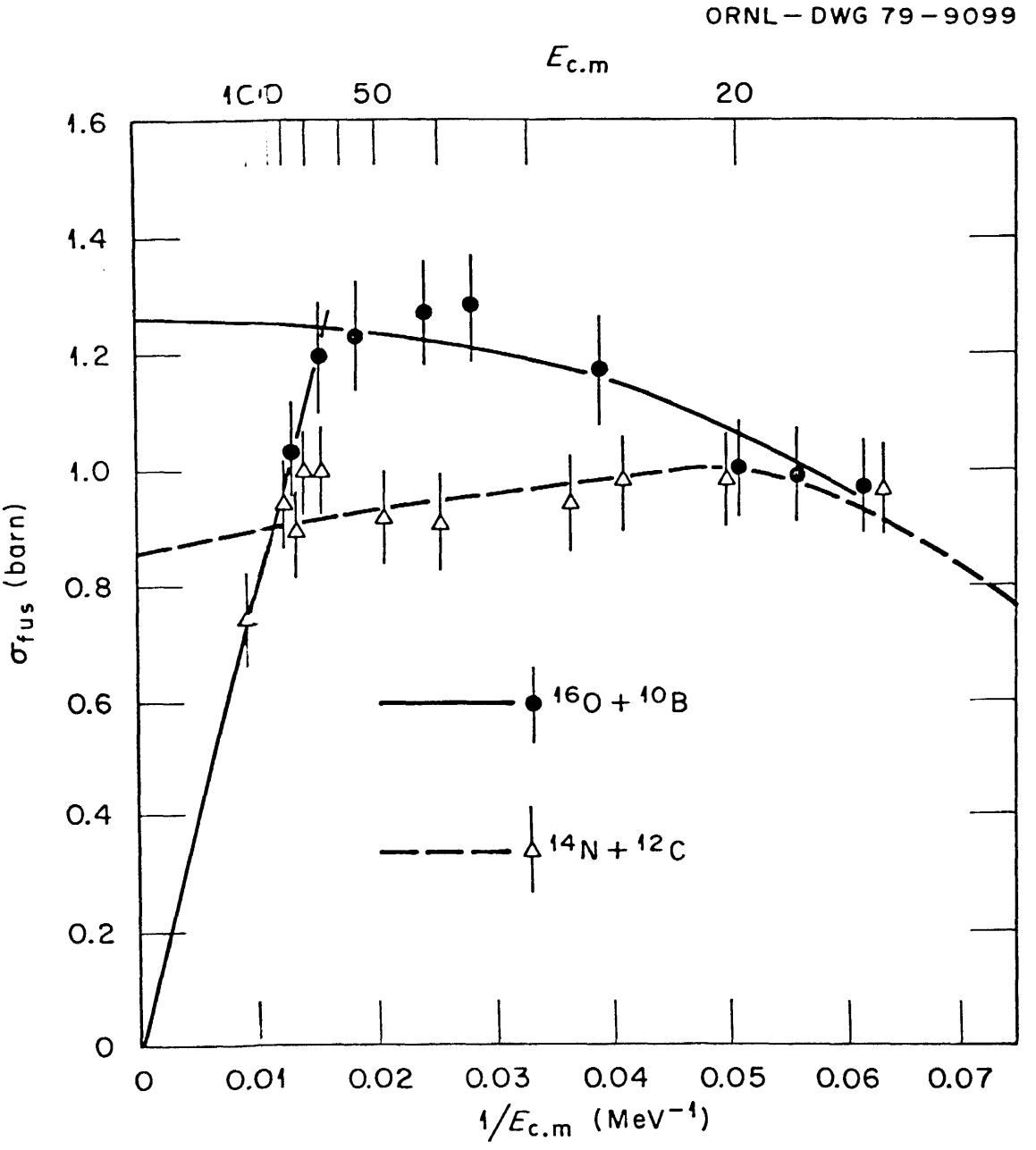
ORNL – DWG 79 – 9099
$E_{c.m}$
100
50
20
1.6
1.4
1.2
1.0
0.8
0.6
0.4
0.2
0
σ_{fus} (barn)
$^{16}O + ^{10}B$
$^{14}N + ^{12}C$
0
0.01
0.02
0.03
0.04
0.05
0.06
0.07
$1/E_{c.m}$ (MeV^{-1})

Fig. 2

ORNL-DWG 77-11453

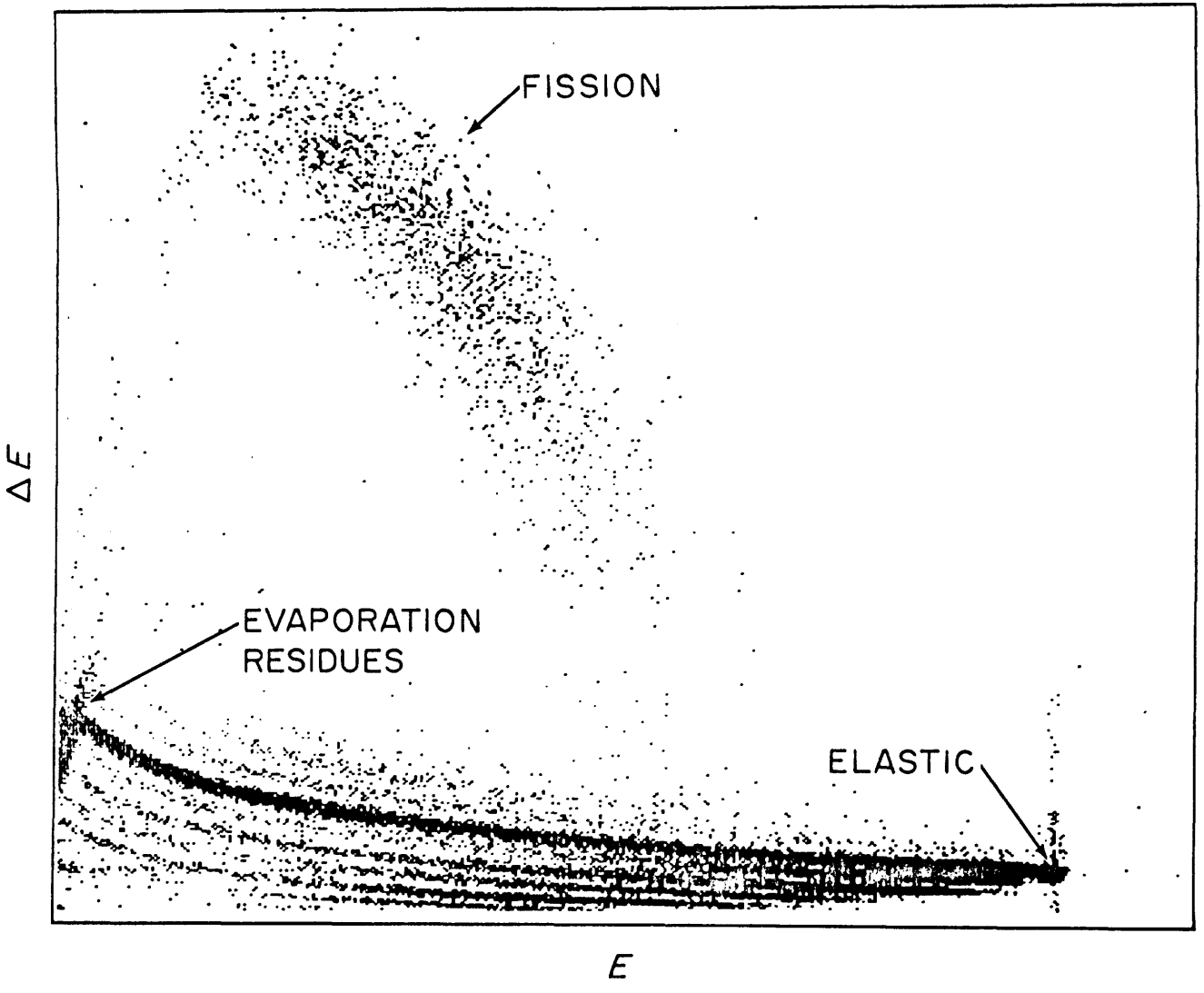

Fig. 3

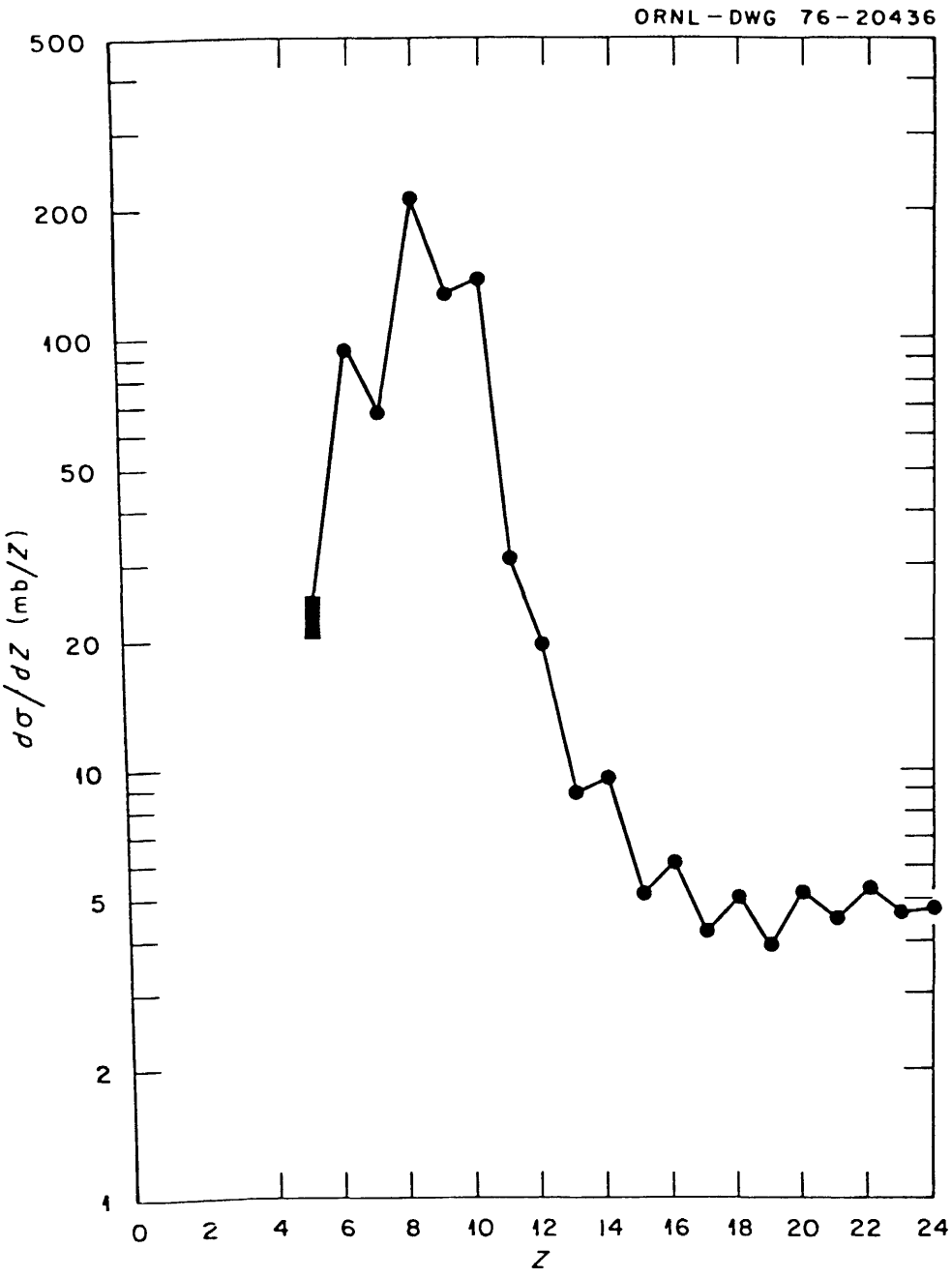
ORNL – DWG 76-20436
500
200
100
50
20
10
5
2
1
dσ/dZ (mb/Z)
0
2
4
6
8
10
12
14
16
18
20
22
24
Z

Fig. 4

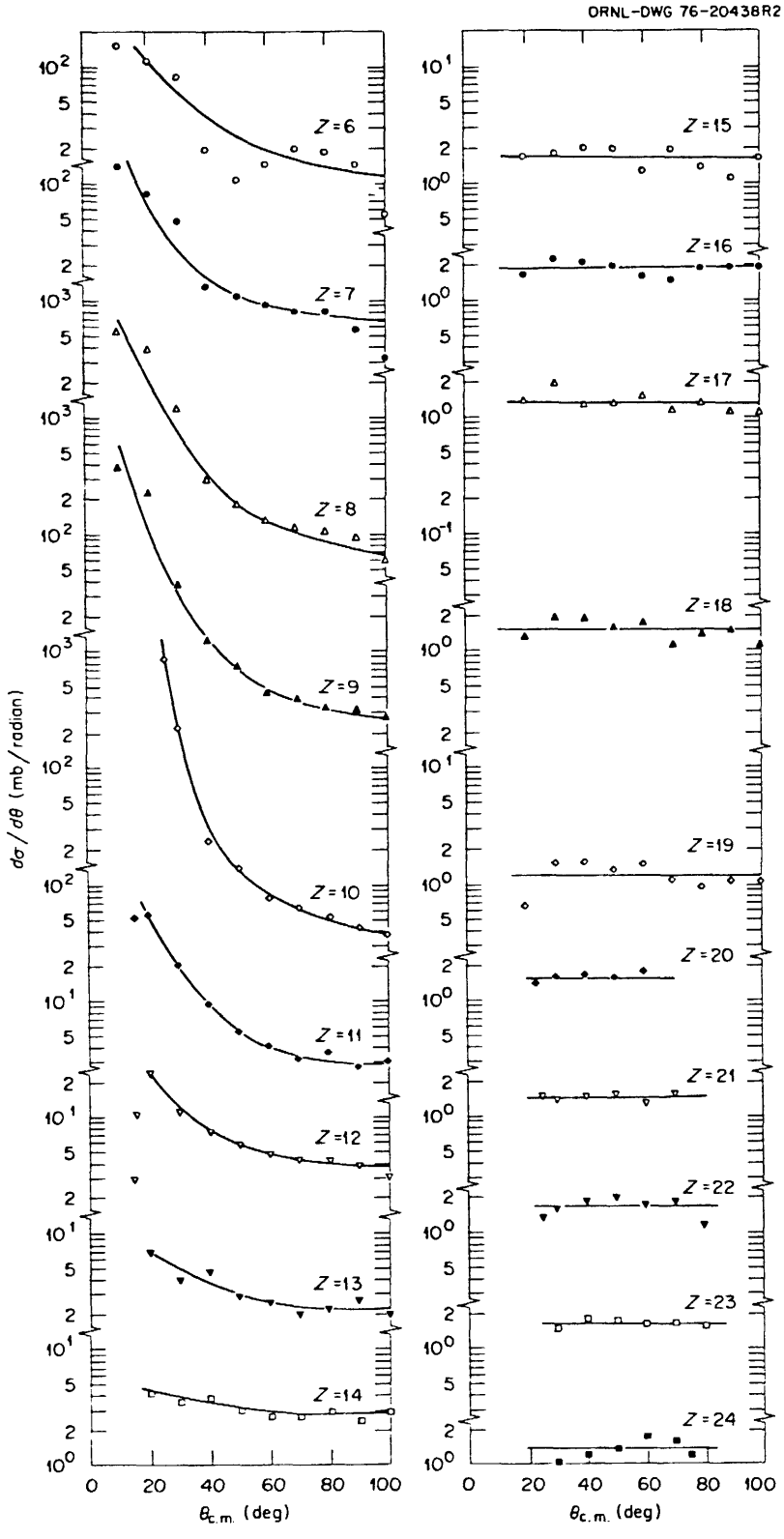
ORNL-DWG 76-20438R2
dσ/dθ (mb/radian)
θc.m. (deg)
θc.m. (deg)
Z=6
Z=7
Z=8
Z=9
Z=10
Z=11
Z=12
Z=13
Z=14
Z=15
Z=16
Z=17
Z=18
Z=19
Z=20
Z=21
Z=22
Z=23
Z=24

Fig. 5

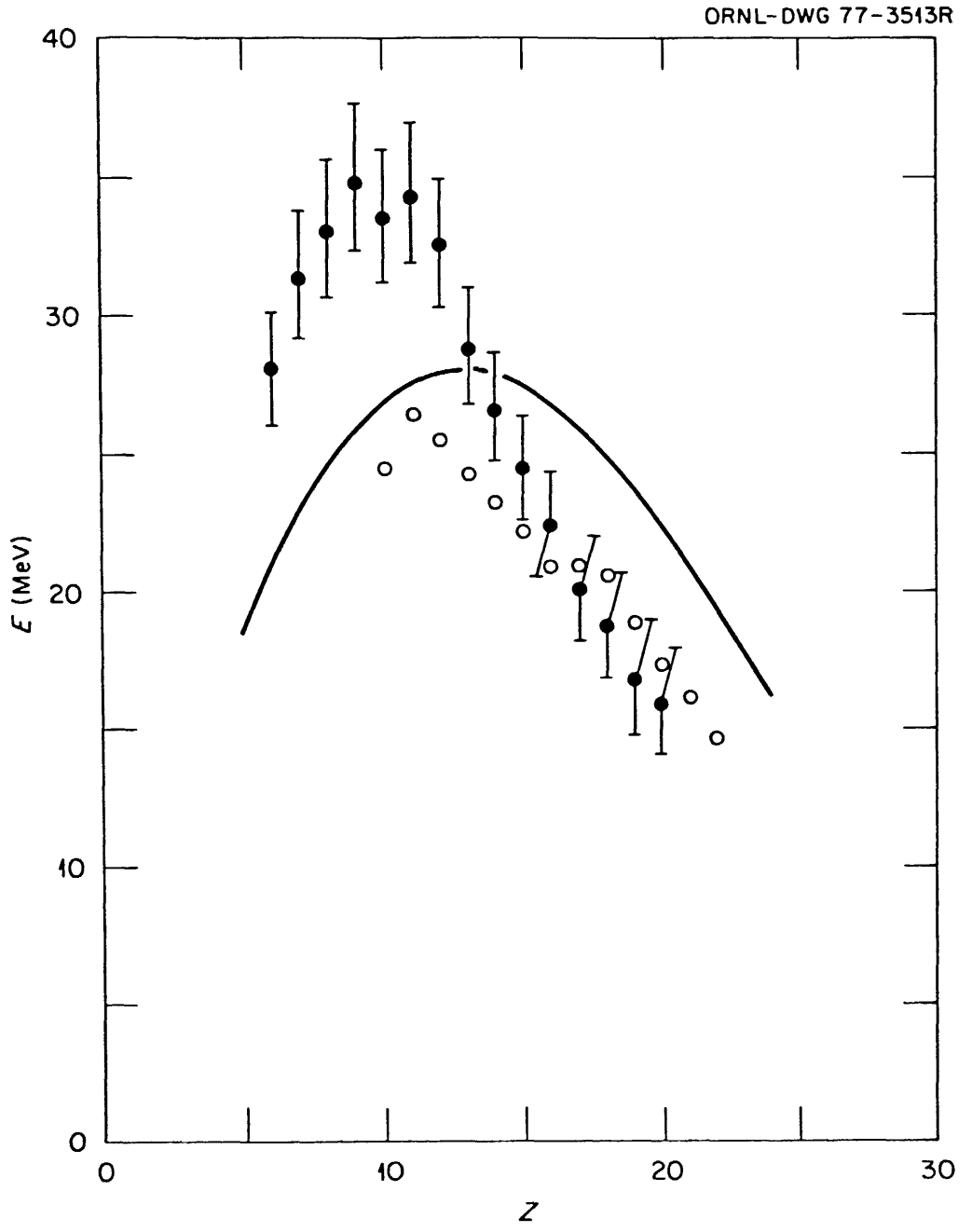

Fig. 6

ORNL-DWG 79-11937

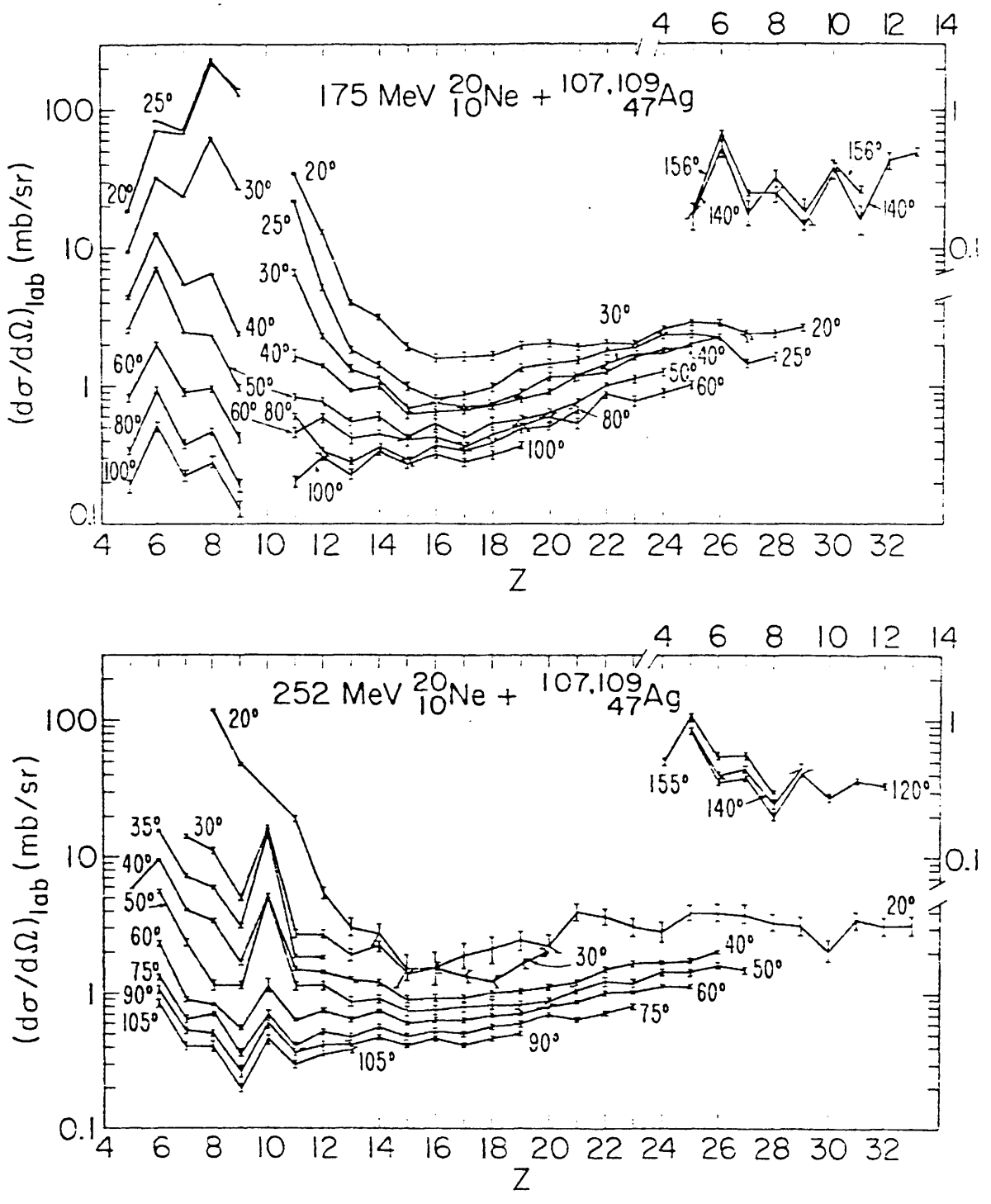

Fig. 7

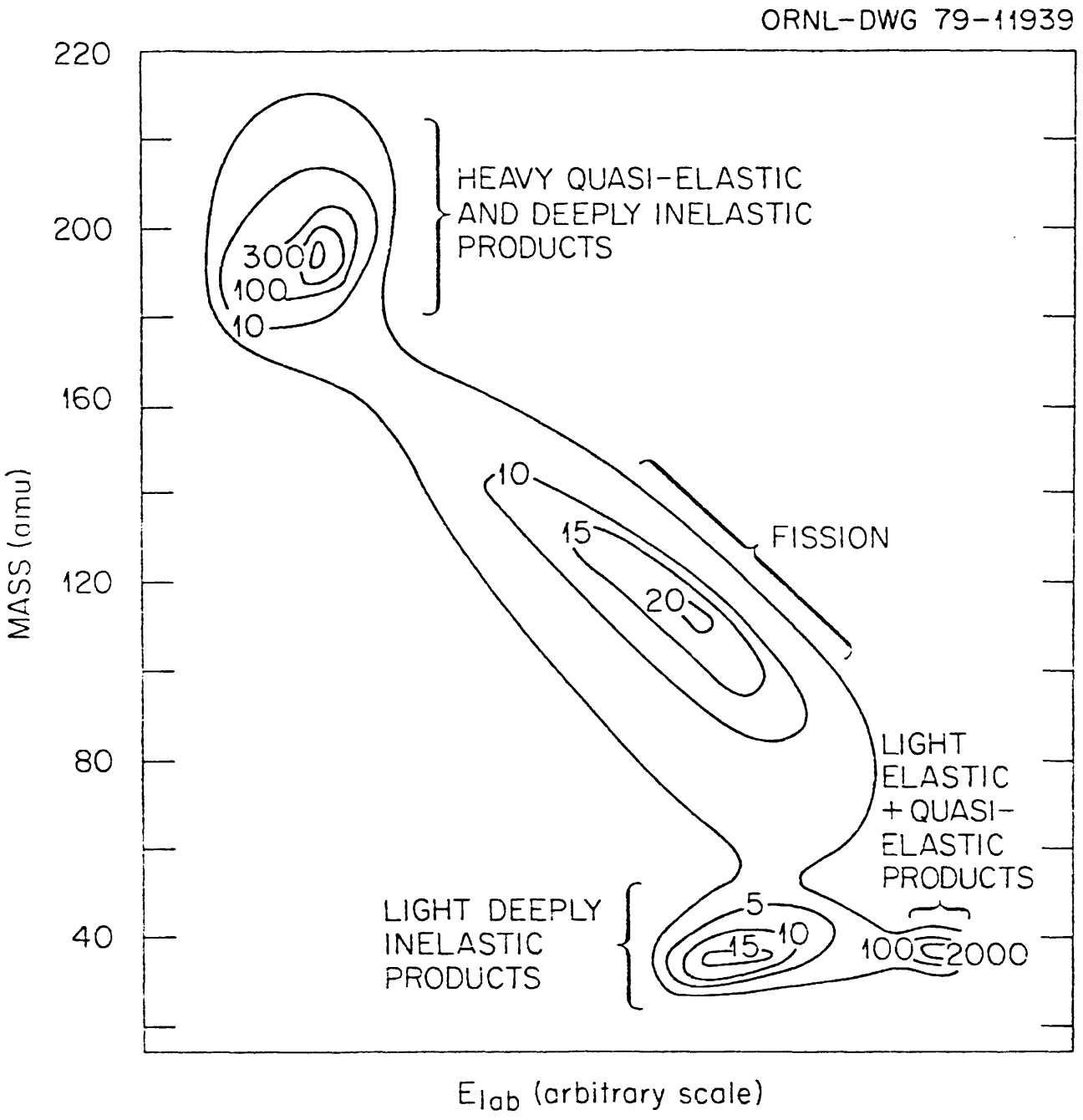
ORNL-DWG 79-11939
220
200
160
120
80
40
MASS (amu)
HEAVY QUASI-ELASTIC
AND DEEPLY INELASTIC
PRODUCTS
3000
100
10
10
15
20
FISSION
LIGHT
ELASTIC
+ QUASI-
ELASTIC
PRODUCTS
LIGHT DEEPLY
INELASTIC
PRODUCTS
5
15
10
100
2000
E_{lab} (arbitrary scale)

Fig. 8

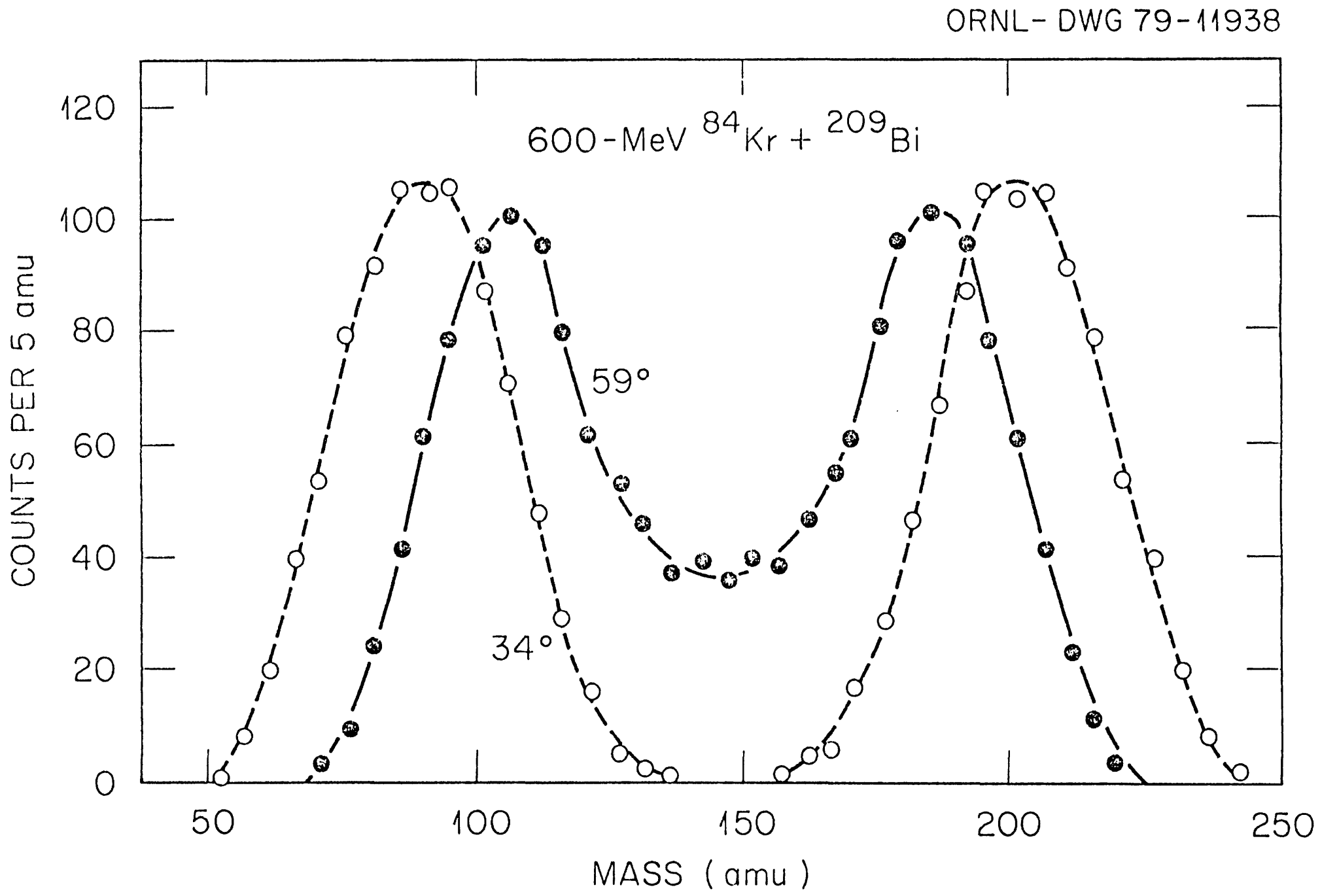
ORNL- DWG 79-11938
600-MeV ^{84}Kr + ^{209}Bi
59°
34°
COUNTS PER 5 amu
MASS (amu)
0
20
40
60
80
100
120
50
100
150
200
250

Fig. 9

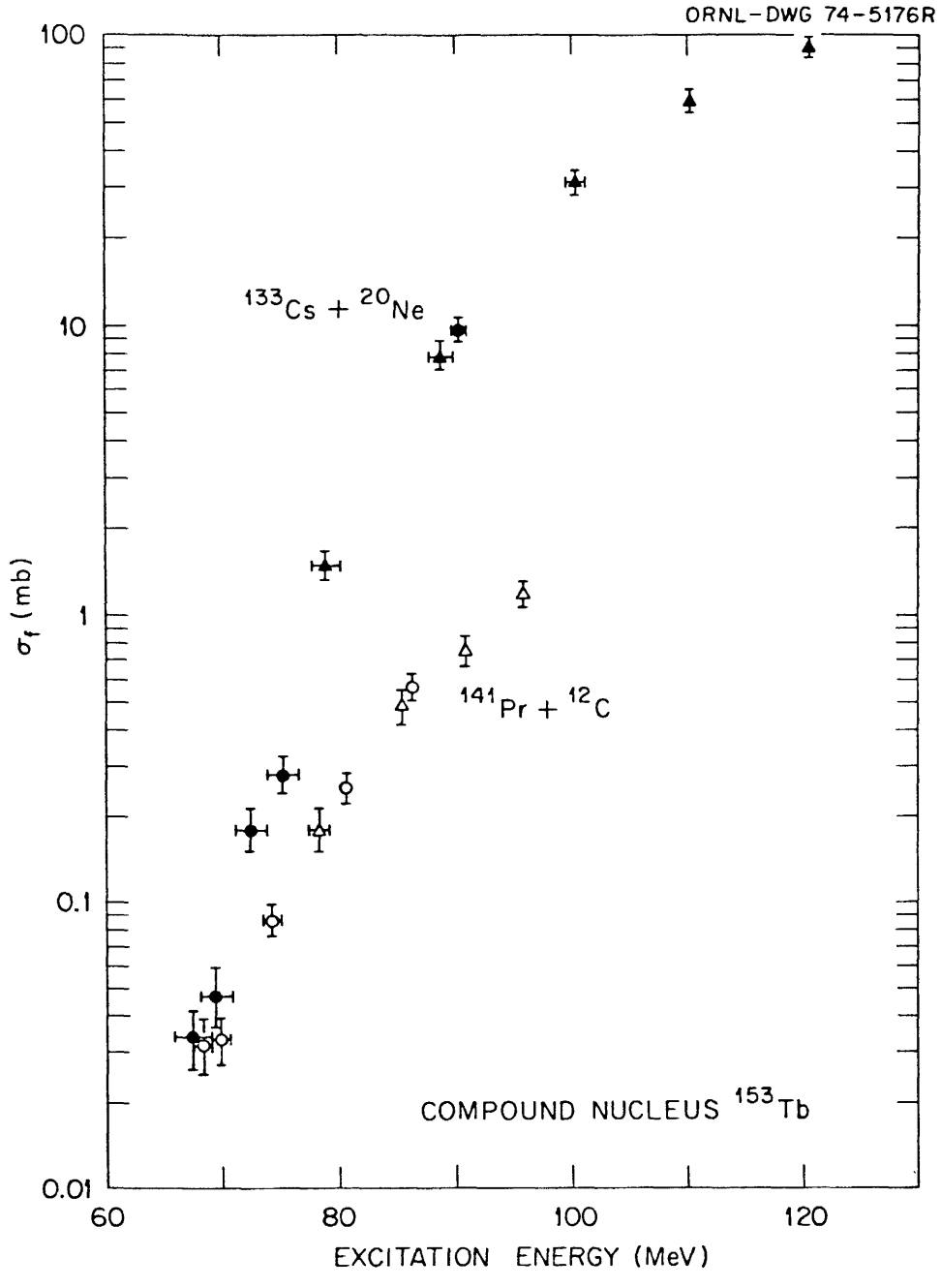
ORNL-DWG 74-5176R
100
10
1
0.1
0.01
σ_f (mb)
$^{133}Cs + ^{20}Ne$
$^{141}Pr + ^{12}C$
COMPOUND NUCLEUS ^{153}Tb
60
80
100
120
EXCITATION ENERGY (MeV)

Fig. 10

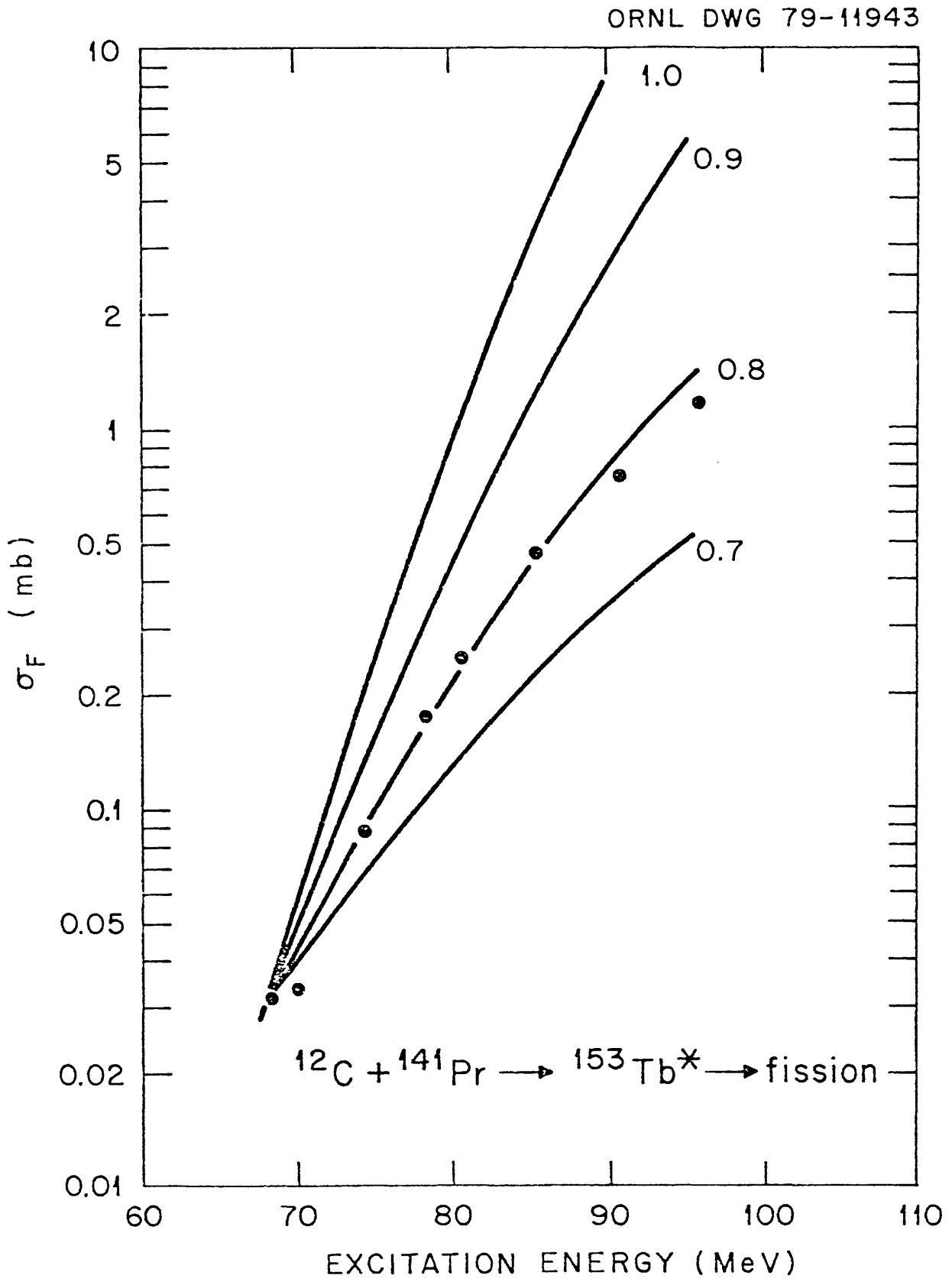
ORNL DWG 79-11943
10
5
2
1
0.5
0.2
0.1
0.05
0.02
0.01
σ_F (mb)
1.0
0.9
0.8
0.7
$^{12}C + ^{141}Pr \rightarrow ^{153}Tb^* \rightarrow$ fission
60
70
80
90
100
110
EXCITATION ENERGY (MeV)

Fig. 11

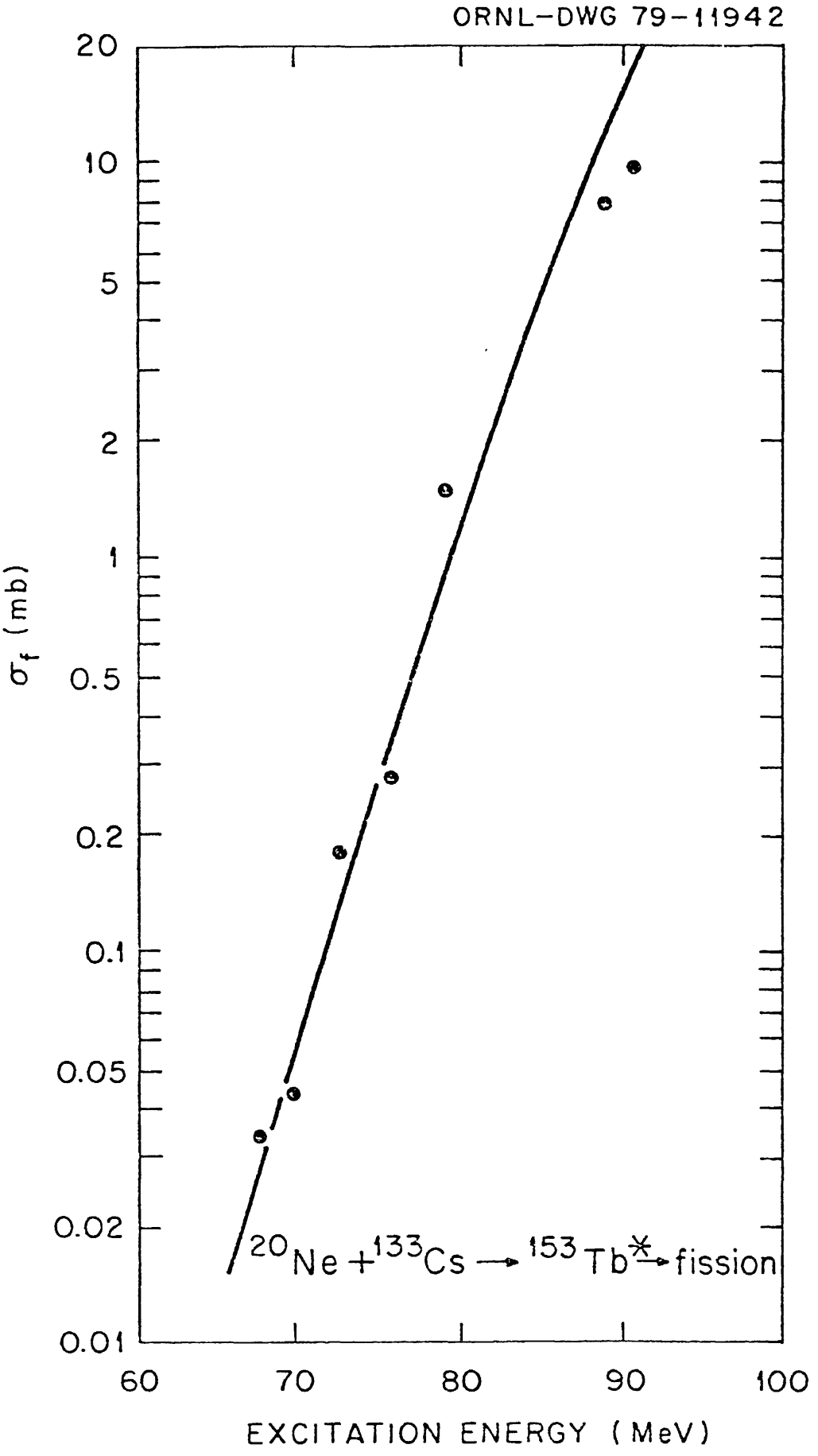
ORNL-DWG 79-11942
20
10
5
2
1
0.5
0.2
0.1
0.05
0.02
0.01
σ_f (mb)
$^{20}Ne + ^{133}Cs \rightarrow ^{153}Tb^{*} \rightarrow$ fission
60
70
80
90
100
EXCITATION ENERGY (MeV)

Fig. 12

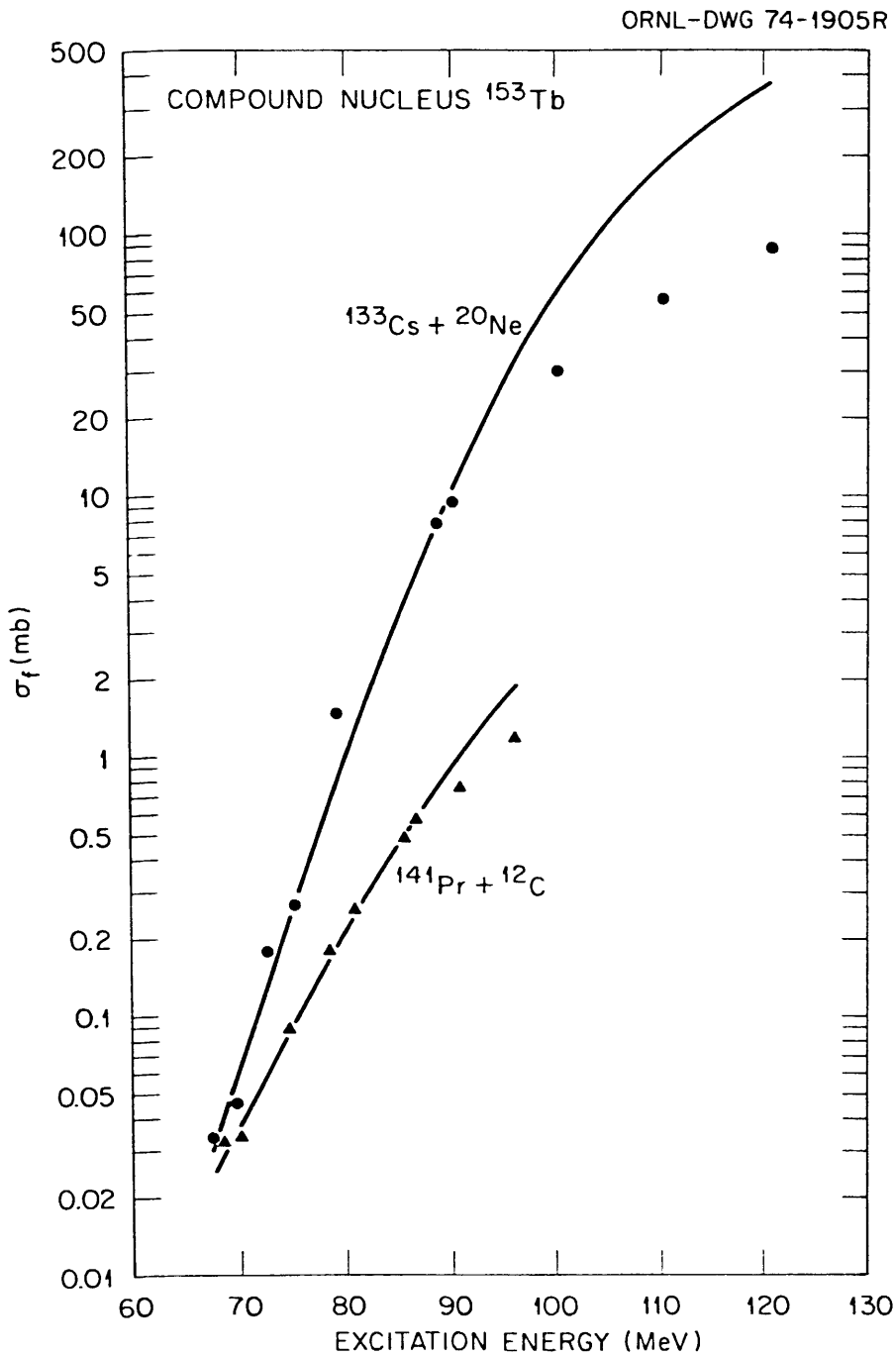
ORNL-DWG 74-1905R
COMPOUND NUCLEUS ^{153}Tb
^{133}Cs + ^{20}Ne
^{141}Pr + ^{12}C
σ_f (mb)
500
200
100
50
20
10
5
2
1
0.5
0.2
0.1
0.05
0.02
0.01
60
70
80
90
100
110
120
130
EXCITATION ENERGY (MeV)

Fig. 13

ORNL-DWG 79-11941

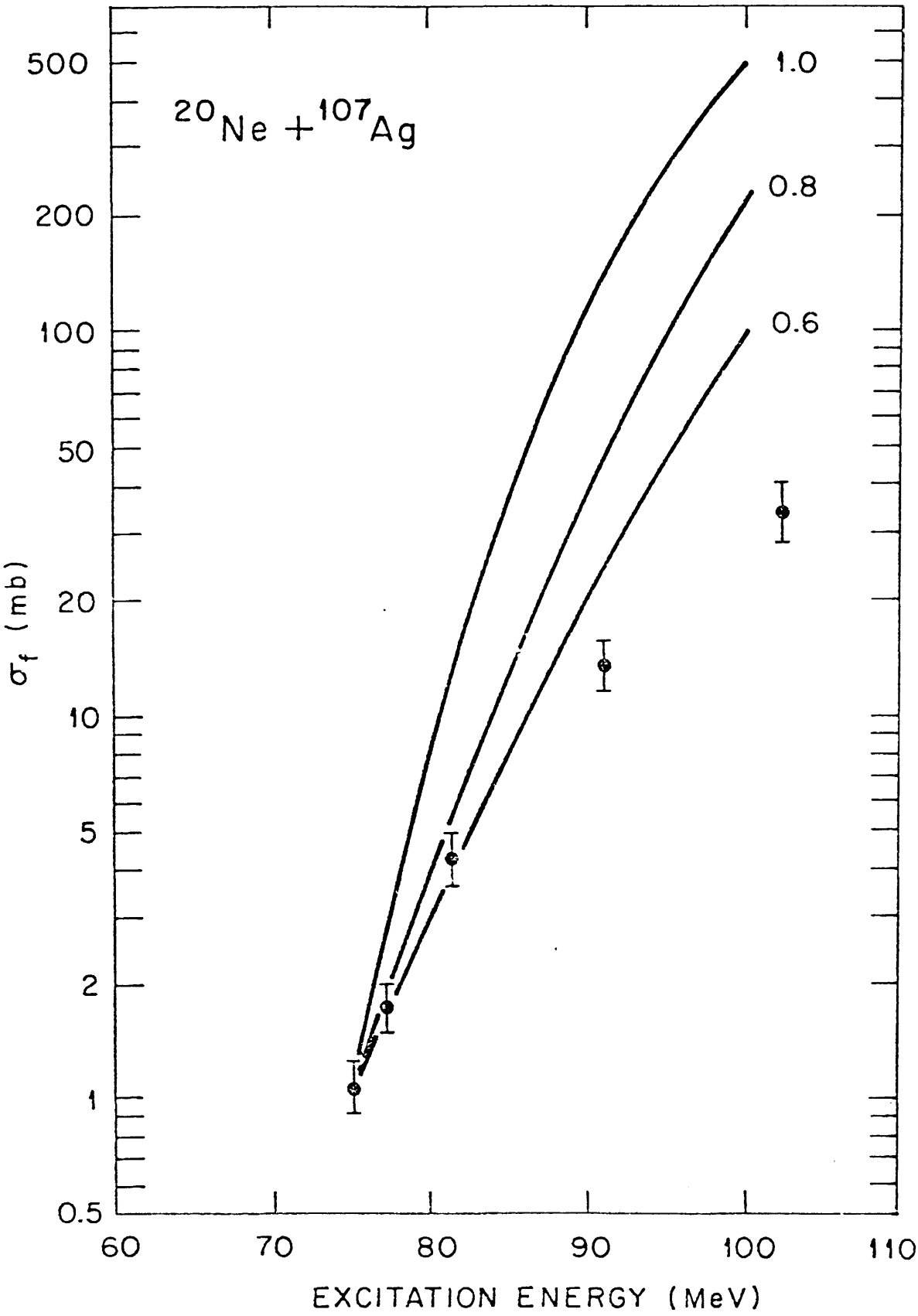

Fig. 14

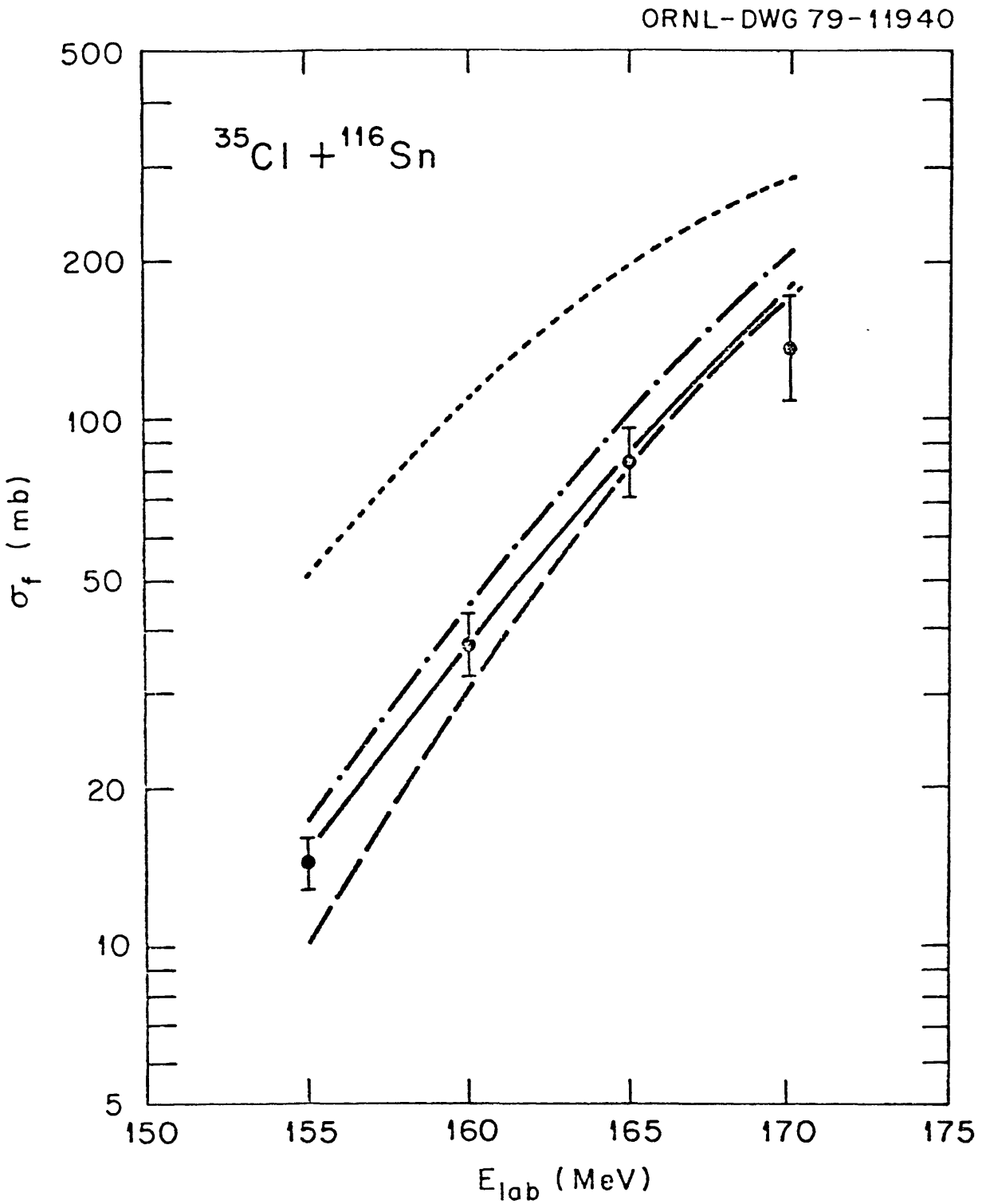
ORNL-DWG 79-11940
$^{35}Cl + ^{116}Sn$
500
200
100
50
20
10
5
σ_f (mb)
150
155
160
165
170
175
E_{lab} (MeV)

Fig. 15